JOURNAL OF CATALYSIS 43, 292–303 (1976)

Chemical, Surface and Catalytic Properties of Nonstoichiometrically Exchanged Zeolites

R. A. SCHOONHEYDT, L. J. VANDAMME, P. A. JACOBS, AND J. B. UYTTERHOEVEN

Centrum voor Oppervlaktescheikunde en Colloïdale Scheikunde, Katholieke Universiteit Leuwen, De Croylaan 42, B-3030 Heverlee, Belgium

Received September 12, 1975; revised January 2, 1976

Zeolites X and Y have been exchanged with Ni^{2+} and Cu^{2+} cations in the presence and absence of acetic acid/acetate buffer, at different ratios of the solid and liquid phases, at different concentrations of the exchange solution, and using successive exchange treatments with fresh solution applying an intermediate treatment or not. Analytical data about the composition of the solid phase have been collected. Well-selected samples have been dehydrated and characterized by TGA, DTA, X-ray diffraction, ir spectra of the hydroxyl groups and of adsorbed CO and CO_2. The catalytic activity of the samples was investigated for the decomposition of isopropanol and the oxidation of carbon monoxide. Together with the exchange of transition metal ions, protons are exchanged and hydroxylated species of transition metal cations are precipitated in the zeolite giving rise to an excess amount of transition metal. The extent to which all this occurs depends strongly on the manner the samples have been prepared. Application of the above-mentioned physicochemical techniques shows the presence of polynuclear species related in some way to the corresponding hydroxide and oxide. The species are mainly located in the supercages. The catalytic properties of the samples confirm the physicochemical characterization.

INTRODUCTION

Ione *et al.* (*1*) and Maksimov *et al.* (*2*) presented ample evidence that different catalysts could be obtained after ion exchange of synthetic zeolites with transition metal ions, depending on the exchange conditions. If the ion exchange was performed at pH values where hydrolysis of the transition metal cations could be expected, polynuclear cation complexes precipitated on the solid. They were characterized by typical ESR and ir spectra, magnetic susceptibility values and catalytic activities comparable to those of the pure oxides of the transition metal cations. At lower pH the ion exchange resulted in a zeolite loaded with transition metal cations dispersed in monomeric form. In the latter case protons can be introduced too, giving rise to acidic properties. It is clear that in order to compare catalytic activities of zeolites exchanged with transition metal cations, the method of preparation of the catalyst and its chemical composition are of the uttermost importance.

This paper aims to rationalize the ion exchange, surface properties and catalytic activities of zeolitic catalysts, loaded with transition metal cations under different conditions.

EXPERIMENTAL PROCEDURES

Preparation of Catalysts

The ion exchanges were performed on Linde synthetic zeolites NaX (lot No. 1340070) and NaY (lot No. 3607-411) after saturation in excess NaCl solution. The cation exchange capacity (CEC) of these samples was 6.25 and 4.25 equiv kg^{-1},

respectively. The reagents were analytical grade $NiCl_2 \cdot 6H_2O$ and $CuCl_2 \cdot 2H_2O$. The standard conditions for the ion exchange experiments were 1 dm^3 0.1 *N* Ni^{2+} or Cu^{2+} solution, 6×10^{-3} kg zeolite and 8.64×10^4 s (24 hr) exchange time at room temperature. These conditions were systematically changed by varying the following factors: (i) pH; (ii) total molarity of the sodium acetate–acetic acid buffer; (iii) temperature; (iv) Ni^{2+}- or Cu^{2+}-concentrations in solution; (v) solid/liquid ratio; (vi) the number of subsequent exchanges. The pH values of the solutions were measured before and after exchange. For exchange with buffered solutions, the Na^+ zeolites were first equilibrated with the buffer, centrifuged and then the buffered solution was added. Water at the same pH as the exchange solution was used for washing until Cl^--free. All the chemical analyses were performed on the solid and included the determination of the water content by calcination at 1073 K in air until constant weight and of the Na^+ and transition metal cation contents by atomic absorption spectroscopy. In some cases Cu^{2+} and Ni^{2+} were determined by EDTA complexometric titration. Both methods gave the same results. $1–2 \times 10^{-3}$ kg of selected samples were repeatedly (4×) back exchanged with 1 dm^3 0.01 *N* Ag^+ at room temperature for 8.64×10^4 s (24 hr) and analyzed for Cu^{2+} or Ni^{2+}, Na^+ and Ag^+ by atomic absorption spectrometry. Back exchange was also performed with Na^+ and TG–DTG–DTA curves were obtained on these samples.

Methods

The samples were characterized by their X-ray diffraction pattern and their TG, DTG and DTA spectra from room temperature up to 1273 K. The latter were obtained in a Mettler thermoanalyzer on $\sim 2.5 \times 10^{-5}$ kg material in a N_2 flow of 1.67×10^{-4} dm^3 s^{-1} at a heating rate of 0.25 K s^{-1} with Al_2O_3 as reference. Selected samples were pressed into wafers of $4–8 \times 10^{-2}$ kg m^{-2}, dehydrated under vacuum at 623 K in the ir spectrometer (Beckman IR12) and their spectra recorded before and after admission of CO and CO_2 in the regions 1200–1800 cm^{-1}, 2000–2400 cm^{-1} and 3000–3800 cm^{-1}.

The catalytic activity for isopropanol decomposition of selected samples was determined in a flow reactor operating in the differential mode. Rates of formation

TABLE 1

Na^+ Release and Ni^{2+} Content, DTA Data and Method of Preparation of Ni-Zeolites in the Presence of Na Acetate–Acetic Acid Buffer

Sample	Na^+ released (% of the CEC)	%		pH	Procedure	DTA	
		Ni^{2+}	$Ni^{2+}+Na^+$			Endotherm (K)	Exotherm (K)
NiY1	60.47	61.18	100.71	5	Standard	443 501	1193
NiY2	20.71	22.12	101.41	6	Standard	—	—
NiY3	21.18	26.12	104.94	7	Standard	458 493	1158
NiY4	63.06	59.76	96.71	5	10^{-3} kg dm^{-3}	—	—
NiY5	57.41	57.41	100.00	6	10^{-3} kg cm^{-3}	—	—
NiY6	37.18	46.35	109.18	7	10^{-3} kg dm^{-3}	—	—
NiY7	50.82	60.94	110.12	6.64	0.01 *M* buffer	—	—
NiX1	68.80	43.52	74.72	5	Standard	393 461	1033
NiX2	61.44	70.56	109.12	6	Standard	—	—
NiX3	59.84	72.00	112.16	7	Standard	493	1063

TABLE 2

Na^+ Release, Ni^{2+} Content and DTA Data of the Catalysts after Exchange in the Absence of Buffer under Different Conditions

Sample	Na^+ released (% of the CEC)	%		pH; exchange:		Procedure	DTA			
		Ni^{2+}	$Na^+ + Ni^{2+}$	Before	After		Endotherm (K)			Exotherm (K)
NiY9	64.00	66.82	102.82	7.10	6.19	pH adjusted with NaOH	458	493		1158
NiY9′	68.00	85.18	117.18	7.13	5.20	NaOH, 359 K	~511	683		1208
NiY10	64.24	82.59	118.35	5.36	6.08	Standard	~513	675		1193
NiY12	65.65	83.06	117.41			0.01 *N* Ni^{2+}				
NiY12′	65.41	91.29	125.88			363 K	~505	673		1198
NiY13	70.59	83.09	112.47			1.2×10^{-2} kg dm^{-3}; 0.5 *N* Ni^{2+}, 363 K				
NiY13′	79.76	90.59	110.82			1.2×10^{-2} kg dm^{-3}; 0.5 *N* Ni^{2+}, 363 K				
NiY13″	81.41	105.65	124.24			1.2×10^{-2} kg dm^{-3}; 0.5 *N* Ni^{2+}, 363 K	453	498	663	1208
NiX5	63.36	64.64	101.28	6.96	6.06	pH adjusted with NaOH				
NiX5′	89.12	94.88	105.92	7.02	5.76	NaOH; 363 K	383	458		1153
NiX6	52.64	47.36	110.72	5.36	6.30	Standard				
NiX6′	91.84	94.72	102.88	5.36	5.28	363 K	388	458		1148

of propylene (r_1), diisopropyl ether (r_2) and acetone (r_3) (mole kg^{-1} s^{-1}) were obtained at 373 K using a flow rate of 1×10^{-3} dm^3 s^{-1}. The composition of the feed was usually 2.667×10^3 N m^{-2} (20 mm Hg) isopropanol in 9.866×10^4 N m^{-2} (740 mm Hg) helium. Carbon monoxide oxidation was also used as a test reaction over the Cu-exchanged samples. The reaction was carried out in a circulation system; the carbon dioxide formed was trapped out and the pressure drop followed with a Texas Instruments precision pressure gauge. The initial composition of the feed was 1.333×10^3 N m^{-2} (10 mm Hg) CO in 1.800×10^4 N m^{-2} (135 mm Hg) O_2. The initial rates of the reaction were calculated at 658 K.

RESULTS

Preparation and Characterization of the Samples

1. *Ni^{2+}-Exchange in the Presence of Acetic Acid–Acetate Buffer*

Table 1 contains the exchangeable cation content of the samples after exchange under different conditions as indicated. The common characteristic of the samples is that the exchange levels calculated from the residual Na^+ content are less than the amount of Ni^{2+} found on the solid. The reverse is true for exchange at pH 5 on X (NiX1), while for Y at pH 5 and 6 the exchange reactions are nearly stoichiometric, i.e., the amount of Ni^{2+} on the solid equals the amount of Na^+ lost within experimental accuracy (NiY4, NiY5). The significant difference between X and Y are the low exchange levels on Y at pH 6 and 7 (NiY2, NiY3) with respect to those found on X exchanged in the same conditions (NiX2, NiX3). However, the exchange limits of Ni^{2+} on Y at pH 6 and 7 can be increased by reducing the solid-liquid ratio (NiY5, NiY6) or the amount of buffer (NiY7).

All the samples are X-ray crystalline. Water loss on NiY occurs with two endothermic peaks in the region 443–458 K and 493–508 K, respectively. Loss of structure is clearly dependent on the amount of Ni^{2+} present as shown by the temperature

dependence of the DTA exotherm (Table 1). Water loss on X is dependent on the mode of preparation with maxima around 393 and 493 K or only one around 493 K (Table 1).

2. Ni^{2+}-Exchange in the Absence of Buffer

The analytical data are presented in Table 2. NiY9-9′, NiY12-12′, NiY13-13′-13″ denote repeated exchanges in identical conditions except when indicated otherwise. The samples NiY13 and NiY13′ underwent an overnight heat treatment under vacuum at 623 K in deep bed conditions before the second and third exchange took place. For NiX5-5′ and NiX6-6′ the same remarks hold. As for the exchange in the presence of a buffer, the exchange levels, calculated from the residual Na^+ content, are lower than the Ni^{2+} content of the zeolites, except for NiX6. We call the difference "excess" Ni. The data indicate that the excess Ni is monitored by the exchange conditions. This leads to the following observations, emerging from Table 2.

i. The excess is more pronounced for Y- than for X-type zeolites.

ii. The exchange level is always higher without buffer than in the presence of buffer in otherwise the same conditions.

iii. The solid acts as a buffer: the pH of 7 is decreased to $\sim 6.10 \pm 0.10$ and the pH of the 0.1 N $NiCl_2$ solution of 5.36 is increased to ~ 6.0 after exchange.

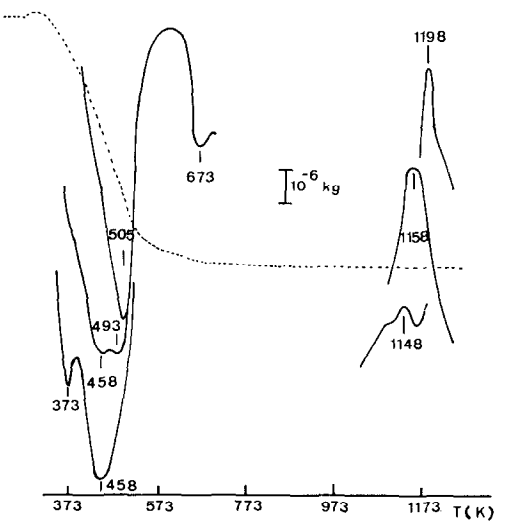

FIG. 1. DTA curves (——) for Ni-zeolites: lower, NiX6′; middle, NiY9; upper, NiY12′. The weight loss curve (– – –) is that of NiY12′ (initial weight: 3.03×10^{-5} kg).

iv. Repeated exchanges only slightly decrease the Na^+ level of the Y-type zeolites (Y9-9′, Y12-12′) but significantly increase the Ni^{2+} level, thus leading to a larger nonstoichiometric part. This is not the case for X-type zeolites where repeated exchanges decrease the Na^+ level significantly and only slightly increase the amount nonstoichiometric Ni (X5-5′, X6-6′).

v. Intermediate heating between two exchanges (623 K, vacuum, 5.76×10^4 s)

TABLE 3

Na^+ Release, Cu^{2+} Content and DTA Data of Zeolite Y, Exchanged under Different Conditions

Sample	Na^+ released (% of the CEC)	%		pH; exchange:		Procedure	DTA				
		Cu^{2+}	$Cu^{2+} + Na^+$	Before	After		Endotherm (K)				Exotherm (K)
CuY1	75.06	89.41	114.59	4.59	4.32	2×10^{-3} kg dm^{-3}	423	493	623		1116
CuY2	63.29	65.88	102.59	4.60	4.64	2×10^{-2} kg dm^{-3}	423	485			1160
CuY2′	69.41	82.35	112.71	4.57	4.12	2×10^{-2} kg dm^{-3}	423	489	609		1149
CuY2″	70.82	108.47	137.88	4.57	4.02	2×10^{-2} kg dm^{-3}	423	478			1153
CuY3	67.29	79.29	112.00	4.59	4.37	10^{-2} kg dm^{-3}	423	497	615		1133
CuY3′	78.12	94.59	116.47	4.32	4.13	Intermediate heating at 673 K under 10^{-4} Torr	423	483	613		1158
CuY3″	85.18	108.47	123.53	4.40	4.19	Intermediate heating at 673 K under 10^{-4} Torr	419		611		1097
CuY4	69.65	72.94	103.29	5.15	5.27	10^{-3} kg dm^{-3}; 0.01 N Cu^{2+}	426	488			1185
CuY5	73.18	217.41	244.47	2.92	3.00	5×10^{-3} kg dm^{-3}; 1 N Cu^{2+}	415		617		952
CuY6	93.88	149.41	155.53	—	—	Reflux	438	508	608	953	1113

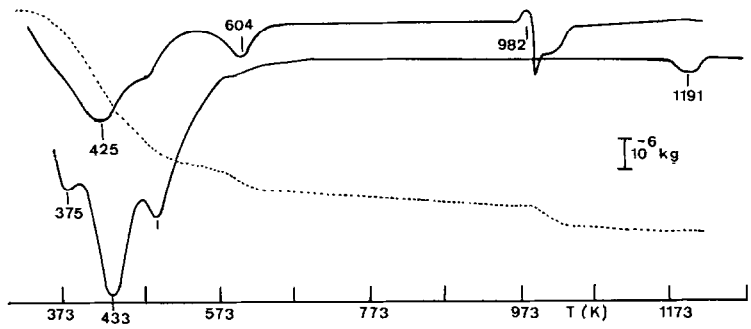

FIG. 2. DTA curves (——) of CuY2 (lower) and CuY5 (upper). The weight loss curve (– – –) is that of CuY5 (2.54×10^{-6} kg initial weight).

leads to high exchange levels for Y zeolites (13-13′-13″), although the third exchange brings only excess Ni on the zeolitic phase.

All the samples prepared are crystalline, when judged from their X-ray diffractograms. The lattice stability and water loss occur in the same temperature ranges as for the samples prepared in the presence of the acetic acid/acetate buffer. Some examples are shown in Fig. 1. At ~90% Ni^{2+} exchange the lattice stability of X-type zeolites is ~100 K higher than at ~70% exchange (Tables 1 and 2).

Every Y-type zeolite with excess transition metal has a supplementary endothermic loss peak at 673 ± 10 K. The corresponding weight loss amounts to ~1% of the total sample weight (Fig. 1).

3. Cu^{2+}-Exchange on Y-Type Zeolites in the Absence of Buffer

Deviations from standard exchange conditions are indicated in Table 3 together with the results of the chemical analyses and the DTA data. As was the case for Ni^{2+}, the nonstoichiometry is more a rule than an exception. The samples CuY1-2-3 and 5 show clearly how the increase of the solid–liquid ratio decreases the exchange level measured from the residual Na^+ content, although the Cu^{2+} content of the solution exceeded the amount necessary for complete exchange. The effects of repeated exchange and intermediate heating between two successive exchanges are similar to those observed for the Ni samples. Finally, we draw attention to the samples CuY5 and CuY6, exchanged in 1 *N* $CuCl_2$ and under reflux, respectively: in both cases the nonstoichiometric Cu is predominant. The samples CuY3″ and CuY5 were also analyzed for their Si/Al ratios. They were found to be 2.63 and 3.06, respectively, thus significantly higher than the 2.5 for the original NaY.

All these Cu^{2+} zeolites were X-ray crystalline and no supplementary crystal-

TABLE 4

Exchangeable Cation Content of Ni- and Cu-Exchanged Zeolites after Back Exchange with Ag^+

Sample	Original (equiv kg^{-1})			Back exchanged (equiv kg^{-1})			
	Na^+	M^{2+}	$Na^+ + M^{2+}$	Ag^+	Na^+	M^{2+}	$Ag^2 + Na^+ + M^{2+}$
NiX6	2.96	3.96	6.92	6.21	0.02	0.42	6.65
NiY9′	1.36	3.62	4.98	3.88	0.01	0.86	4.75
CuY2′	1.30	3.50	4.79	4.08	0.04	0.58	4.70
CuY2″	1.24	4.61	5.86	3.74	0.03	0.94	4.71
CuY4	1.29	3.10	4.39	3.98	0.02	0.36	4.36

line phase could be detected on the X-ray diffractograms. Only in the case of CuY5 was a CuO phase detected after heating at 633 K in N_2 or in air. X-Ray line broadening techniques revealed the presence of CuO particles with an average diameter of 11 nm. On the other samples, the CuO (and also NiO) phase behaved as amorphous to X-rays. The average particle size was therefore lower than 4 nm (*3*). However, after a 993 K treatment both the CuO and zeolitic phases were destroyed on the CuY5 sample.

The thermogravimetric and DTA data for the Cu zeolites were more complicated than for the Ni samples (Fig. 2). Besides the zeolitic water loss in the 413–493 K region the samples with excess Cu were characterized by an endothermic loss peak at 613 ± 10 K. This weight loss amounted to 1–3%, increasing with increasing amount of nonstoichiometric Cu. Above that temperature a small but continuous weight loss of ~1% was observed. The structural collapse was always associated with an abrupt (~0.5%) weight loss. The samples CuY5 and CuY6 had very characteristic thermograms, also shown in Fig. 2. Besides the 2.4–3% weight loss at 613 K additional weight losses of 2.1% in the region 613–953 K, 2.8% at 953 K and 0.7% in the region 953–1273 K were observed.

4. Back Exchange with Ag^+

Only a few representative samples were investigated and the analytical results are displayed in Table 4. It is clearly shown that the total amount of ions determined after back exchange is always less than before, except for CuY4. In no case was it possible to exchange completely the Ni^{2+} or Cu^{2+} originally present on the solid. The amount remaining on the zeolitic phase is proportional to the excess originally on the solid. Also, the Ag^+ concentration is less than the CEC except for NiX6. After repeated back exchange with Na^+ the DTA curves were different from the original in that the 673 ± 10 K endotherm of Ni was shifted to 603 ± 10 K and the 613

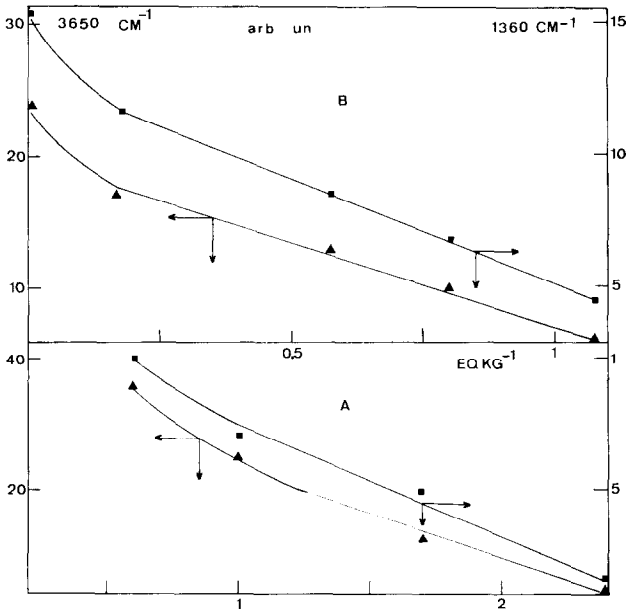

FIG. 3. Relation between the excess transition metal [(Na + Cu) − exchange capacity, both in equiv kg^{-1}] the O_1–H band intensity (3650 cm^{-1}) and the intensity of the 1360 cm^{-1} band of adsorbed carbon dioxide (arbitrary units). (A) Copper and (B) nickel Y sieves.

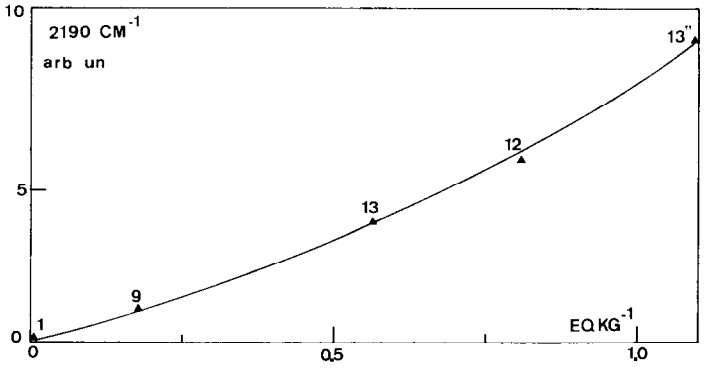

FIG. 4. Relation between the excess Ni (same units) and the band intensity at 2190 cm^{-1} of adsorbed carbon monoxide (arbitrary units).

± 10 K loss of Cu was shifted towards the region 533–563 K. The weight loss associated with these endothermic DTA peaks could not be determined because they were submerged in the background of the zeolitic water loss.

5. *Infrared Spectroscopic Results*

After outgassing *in vacuo* and slowly heating to 623 K most of the samples show hydroxyl bands around 3640–3660 cm^{-1}. On several Ni samples a very weak band at 3680 cm^{-1} is observed. These OH groups are able to protonate ammonia and pyridine. The hydroxyl band intensity is generally more intense on Cu than on Ni-exchanged Y samples, but is still more pronounced on NiX1 and NiX2. Figure 3A and B shows that there exists a smooth relation both for Cu and NiY zeolites between the intensity of the 3650 cm^{-1} band and the excess ions on the solid; when the excess increases, the OH band intensity decreases.

The same relationship exists for the band intensity (1360 cm^{-1}) of adsorbed CO_2 (Fig. 3A and B). When excess Ni is present the intensity of a band at 2190 cm^{-1} is related to this excess (Fig. 4). This band is obtained after room temperature absorption of carbon monoxide and is stable to outgassing temperatures of 373 K. After room temperature adsorption of CO, bands around 2370 and 2350 cm^{-1} are also observed on samples NiY13'', NiX3, CuY5, and CuY6.

6. *Catalytic Activity of Selected Samples*

a. Isopropanol decomposition. In the experimental conditions used, isopropanol is dehydrated via an intermolecular and intramolecular mechanism and also dehydrogenated. The extent to which each process occurs depends on the nature of the catalyst. The rate of formation of the different products: propylene (r_1), diisopropyl ether (r_2) and acetone (r_3) is related to the rate of alcohol decomposition (r_p) as expected from the reaction stoichiometry

$$r_p = r_1 + 2r_2 + r_3.$$

In Fig. 5, the dehydration rate is correlated with the intensity of the 3650 cm^{-1} hydroxyl band. For both Ni- and Cu-containing Y zeolites r_1 and r_2 increase linearly with the optical density of the 3650 cm^{-1} hydroxyls. The relative activity of dehydration is also considerably higher on CuY compared to NiY samples. The OH concentration behaves in the same way. The ratio of the rate of ether and olefin formation remains constant on both series of catalysts. However, the selectivity for intermolecular dehydration [r_2/

$(r_1 + 2r_2)$] is higher on Cu-exchanged zeolites.

The change of the rate of acetone formation (r_3) on CuY and NiY zeolites with increasing "excess" transition metal is shown in Fig. 6. In this figure, the weight loss of the corresponding samples at the high temperature endotherm is considered to be the most exact approximation to the amount of nonstoichiometrically exchanged transition metal. Indeed, the values of $\Sigma(Na^+ + Cu^{2+}$ or $Ni^{2+})$-CEC does not include the extent to which protons are taken up during the exchange reaction. Figure 6 shows a good linear correlation between the rate of dehydrogenation and the weight loss at the high temperature endotherm.

b. Carbon monoxide oxidation. The initial rate of carbon dioxide formation over Cu-containing Y sieves is shown in Fig. 7. It appears that this rate also increases with increasing loading of the CuO phase. The latter parameter is represented again by the weight loss at the high temperature endothermic peak in the thermograms.

DISCUSSION

Ion Exchange in the Presence of Buffer

During the ion exchange of transition metal ions into synthetic zeolites X and Y

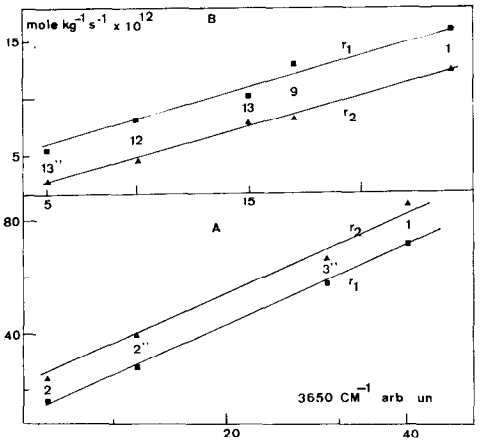

FIG. 5. Increase of the rate of olefin (r_1) and ether formation (r_2) from propan-2-ol on catalysts with increasing amounts of hydroxyls at 3650 cm^{-1}. (A) CuY and (B) NiY.

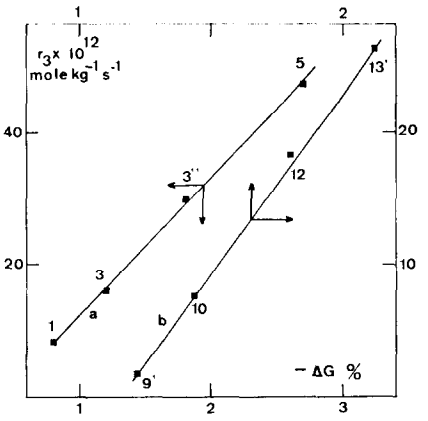

FIG. 6. Relation between rate of acetone formation (r_3) and the percentage weight loss of the catalysts at the high temperature DTA endotherm. (a) Cu and (b) NiY.

the following equilibria are established in solution:

$$Ni^{2+} + Ac^- \rightleftarrows (NiAc)^+, \quad (1)$$

$$(NiAc)^+ + Ac^- \rightleftarrows Ni(Ac)_2, \quad (2)$$

$$NaAc \rightleftarrows Na^+ + Ac^-, \quad (3)$$

$$HAc \rightleftarrows H^+ + Ac^-, \quad (4)$$

$$Ni^{2+} + OH^- \rightleftarrows (NiOH)^+, \quad (5)$$

$$(NiOH)^+ + OH^- \rightleftarrows Ni(OH)_2, \quad (6)$$

$$NaOH\ Na^+ \rightleftarrows + OH^-. \quad (7)$$

In writing these equilibria the formation of polynuclear complexes has been neg-

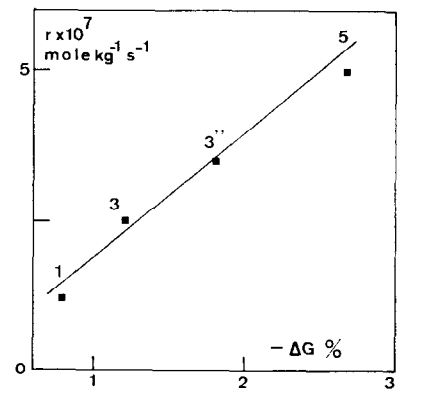

FIG. 7. Relation between the rate of CO oxidation over CuY and the percentage weight loss at the high temperature endotherm.

TABLE 5

Uptake of Ni^{2+}, $(NiAc)^+$ and $Ni(Ac)_2$ (equiv Ni^{2+}/kg Dry Zeolite)

	NiY1	NiY2	NiX2	NiY3	NiY6
Ni^{2+}	1.66	0.55	1.21	0.54	0.28
$(NiAc)^+$	0.81	0.44	2.23	0.17	1.10
$Ni(Ac)_2$	0.13	0.12	0.98	0.07	0.60
CEC-(Ni^{2+} + $(NiAc)^+$) (1)	2.19	3.48	3.92	3.67	3.42
Na^+ on solid (exp.) (2)	1.68	3.37	2.41	3.35	2.67
H^+ = (1) − (2)	0.51	0.11	1.51	0.28	0.75

lected. With the aid of the appropriate equilibrium constants, tabulated by Sillén and Martell (*4*), it is possible to calculate the equilibrium concentrations of the different species before and after ion exchange. A similar calculation, written out in detail, was published by Steger (*5*). From the change in concentration of the different species in solution before and after exchange in standard conditions Table 5 was constructed. It clearly shows that the zeolite has taken up Ni^{2+}, $(NiAc)^+$, and $Ni(Ac)_2$. The concentration of hydroxide species in the presence of the buffer is too low to affect these numbers significantly even at pH 7. The sum of Ni^{2+} and $(NiAc)^+$ should be equal to the amount of Na^+ exchanged in the absence of any other exchange reaction. Table 5 shows that a difference exists, which is especially pronounced for the X-type zeolites. We suggest that the difference is filled up by the uptake of protons. Thus the OH groups, revealed by ir spectroscopy, can be accounted for by acid exchange and not by water dissociation in the electric field of Ni^{2+} ions as suggested for Ca^{2+} and La^{3+} (*6*).

The concentrations of the different species on the zeolites, as given in Table 5, may not be exact because it was assumed that no polynuclear complexes were formed and that the equilibrium constants for reactions (1)–(7) on the solid were the same as in solution. In any case the data of Table 5 qualitatively indicate how the preferential exchange of $(NiAc)^+$ on NiX2 explains the higher exchange levels found on these samples with respect to the corresponding NiY2 (Table 1). The preferential uptake of $(NiAc)^+$ also accounts for the higher exchange level of NiY6 with respect to NiY3, the only difference being a solid–liquid ratio of 1×10^{-3} kg dm^{-3} in the former case and 6×10^{-3} kg dm^{-3} in the latter. We may conclude that the exchange is not only monitored by the concentration of the different ionic species in solution but also by the nature and concentration of the exchanger.

Ion Exchange in the Absence of Buffer

Even in the absence of the buffer the equilibria (5)–(7) lead to too small concentrations of hydroxide species (except for Cu at pH 7) to account for the observed excess. We suggest that polynuclear complexes of the type $M_x(OH)^{+2x-y}$ are formed and ion-exchanged or precipitated on the solid. This is especially likely to occur for Cu (*7*, *8*). The exchanger, however, plays an active role. This is evidenced by the observation that successive exchanges do not increase significantly the exchange level as measured from the residual Na^+ content, of Y-type zeolites, except when intermediate heating has been applied, but they do for X-type zeolites. The result is a larger excess on Y than on X after such a treatment.

Finally, the back exchange experiments (Table 4) and the ir spectroscopic data indicate that protons were exchanged too. This is no surprise in view of the pH of the

exchange solutions, especially for Cu. Also, under severe conditions the Cu exchange leads to some lattice destruction since the Si/Al ratios of the samples CuY3″ and CuY5 increased after exchange.

Characterization of the Excess Transition Metal

From the analysis of the ion exchange data the excess transition metal was attributed to acetate complexes in the case of a buffered exchange and to precipitation and/or ion exchange of hydroxide species during exchange in the absence of buffer. On the basis of ESR and magnetic susceptibility measurements Ione *et al.* (*1*) and Maksimov *et al.* (*2*) came to the same conclusion. The endothermic loss at 673 K for Ni and at 613 K for Cu was only visible in the presence of excess transition metal. It is therefore ascribed to water loss of the hydroxylated transition metal species. The presence of an X-ray detectable CuO phase on CuY5 after heating at 633 K confirms this conclusion. The temperature of 673 K compares favorably with the 603–633 K reported for dehydroxylation of nickel hydroxyde on silica (*9*) and with the 645 K for the decomposition of the mineral $4Ni(OH)_2 \cdot NiOOH$ to NiO (*10*). The decomposition of the $Cu(OH)_2$ and $Ni(OH)_2$ is terminated around 513–523 and 613 K, respectively (*11*). It is therefore quite probable that no pure hydroxide is precipitated on the zeolite. Extensive back exchange gives residual Cu and Ni on the zeolite decomposing in the temperature ranges of the hydroxides. This indicates that repeated contact with the aqueous solution not only dissolves some of the excess (the intensities of the DTA peaks are smaller than those obtained before ion exchange) but also transforms it into pure hydroxide.

Physicochemical Properties of the Samples

The Cu and Ni zeolites X and Y prepared by ion exchange show hydroxyl groups absorbing around 3650 cm^{-1}, generally assigned to O_1–H groups vibrating in the supercages (*6*, *12*, *13*). The analytical data show that most of these hydroxyl groups originate from an ion exchange process and not from dissociation of water molecules under the influence of the electric field of the cations. For both transition metals, the amount of supercage hydroxyl groups declines when "excess" transition metal is present (Fig. 3). This indicates that at least part of the excess is present in the supercages, most probably as a polynuclear complex with a residual positive charge, since it takes the place of protons and cations. In view of this, the small band at 3680 cm^{-1} might be indicative of Ni–OH species (*24*, *25*). The latter statement is confirmed by the ir spectra of adsorbed carbon dioxide molecules. It was pointed out earlier (*14*) that a band in the region 1360–1390 cm^{-1} was due to the ν_1 vibration of CO_2 physisorbed linearly by ion–dipole interaction on polyvalent supercage cations. It seems that also the amount of supercage transition metal cations (Fig. 3) decreases smoothly when the excess transition metal increases.

The presence of increasing amounts of NiO after dehydration of the Ni-exchanged Y zeolites is shown when the amount of

TABLE 6

Selectivity for dehydrogenation of Isopropanol and Brønsted Acidity of the Catalyst

Catalyst	$(S)^a$	O_1–H concn. (relative units)
CuY1	0.100	36
CuY3	0.210	29
CuY3″	0.325	15
CuY5	0.452	05
NiY9′	0.117	19
NiY10	0.290	14
NiY12	0.490	9
NiY13′	0.600	5
NaY70	0.005	—

[a] $S = r_3/(r_1 + r_2 + r_3)$.

excess Ni increases. Indeed, a band at 2190 cm^{-1} of carbon monoxide adsorbed on NiO is generally assigned to the species (*15*, *16*):

$$Ni\cdots O----C\equiv\equiv O.$$

In view of this Fig. 4 shows increasing amounts of the latter species at increasing quantities of excess Ni.

Finally, infrared examination of the samples shows that increasing amounts of excess transition metal are located in the supercages, taking the place of corresponding exchangeable cations and protons. The reactivity of the dehydrated polynuclear Ni species in the zeolite towards carbon monoxide is different from bulk or supported NiO (*17*) due to the lack of surface carbonate.

Catalytic Activity of the Samples

Previous work (*19–22*) on the dehydration of propan-2-ol on zeolites X and Y, clearly shows that protons are the most probable source of the catalytic activity for propylene formation. Recently, it was shown (*18*) that both the intermolecular and intramolecular dehydration activity of propan-2-ol is due to OH groups available in the supercages. Propylene formation requires only one hydroxyl group, while for the formation of diisopropylether a pair of OH groups is needed.

The results presented in this work on Cu- and Ni-exchanged Y zeolites containing an excess amount of transition metal confirm the results of Gentry and Rudham (*18*). Indeed, the rates of propylene and ether formation increase in a way parallel with the supercage hydroxyl groups (Fig. 5). The slope of these lines is higher for the Cu samples containing the higher amounts of O_1–H groups. The ratio of inter- to intramolecular dehydration rate is higher than unity on the CuY catalysts while on the NiY samples this ratio is lower than unity. Therefore, for the samples with the higher O_1–H group population, having also a higher probability to contain pairs of O_1–H groups in the supercages the preferred dehydration is along the intermolecular pathway.

Part of the propan-2-ol molecules are also decomposed via a dehydrogenation reaction, resulting in the formation of acetone. The absolute rate of dehydrogenation increases when the amount of excess transition metal increases (Fig. 6). This is true both for the Cu and the Ni faujasites. From Table 6, it is evident that also the selectivity for dehydrogenation increases when the excess transition metal increases and when the proton concentration in the supercages decreases. This allows us to conclude that the dehydrogenation sites are inherent to the NiO- and CuO-like phases, the major part of which is located in the zeolite supercages. From other work (*23*) it is known that NiO and CuO have no dehydration but considerable dehydrogenation activity.

Maksimov *et al.* (*2*) found that the atomic catalytic activity of Cu in Y zeolites in the carbon monoxide oxidation reaction increased practically up to the level of cupric oxide, when the pH of the exchange solution is increased gradually. The catalytic activity seems to be determined by the degree of cation association and the presence of extralattice oxygen atoms. The results obtained in this work (Fig. 7) confirm the observations of Maksimov *et al.* (*2*). The amount of nonstoichiometrically exchanged copper after dehydration of the sample determines the catalytic activity. However, these data do not allow us to decide about the nature of the active species in this reaction. Further work on this subject is in progress.

CONCLUSIONS

The loading of synthetic faujasites with a maximum of transition metal cation by an ion exchange process shows two major side processes. In the presence of buffer proton exchange occurs together with $(NiAc)^+$ exchange and adsorption of $Ni(Ac)_2$, giving rise to excess transition metal cation on the solid. In the absence of buffer proton exchange is accompanied by exchange

and/or precipitation of hydroxide species of transition metal cations. The extent to which these phenomena occur depend on the type of transition metal cation, the type of zeolite and the exchange conditions. The excess transition metal ion dehydrates in the same temperature region as the corresponding hydroxide. Only when the excess is initially high can an X-ray diffractogram be obtained. Adsorption of CO on the dehydrated zeolite reveals that the excess Ni has some properties in common with NiO, but others are not. Careful examination of the zeolite surface shows that the major part of the excess transition metal is accommodated in the supercages at the expense of supercage protons and transition metal cations.

The catalytic activities for the dehydrogenation of propan-2-ol and the oxidation of carbon monoxide are related to the amount of excess transition metal. The activity for dehydration of propan-2-ol is related to the supercage hydroxyl groups of the type O_1–H. The change of the catalytic activity with the amount of excess transition metal points to the same conclusions as explained in the previous paragraph. All these observations are consistent with the presence of the following species after dehydration:

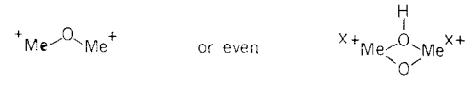

where Me represents Cu or Ni.

ACKNOWLEDGMENTS

R. A. S. and P. A. J. are grateful to N.F.W.O. (Belgium) for a research position as "Aangesteld Navorser". L. J. V. acknowledges a research grant from I.W.O.N.L. (Belgium). Financial support from the Belgian Government (Dienst Wetenschapsbeleid) is gratefully acknowledged. The technical assistance of Mia Tielen, Lieve Leplat and Willy Coopmans is appreciated.

REFERENCES

1. Ione, K. G., Bobrov, N. N., Boreskov, K. G., and Vostrikova, L. A., *Dokl. Akad. Nauk SSSR* **210**, 388 (1973).
2. Maksimov, N. G., Ione, K. G., Anufrienko, V. F., Kuznetsov, P. N., Bobrov, N. N., and Boreskov, G. K., *Dokl. Akad. Nauk SSSR* **217**, 135 (1974).
3. Innes, W. B., *in* "Experimental Methods in Catalytic Research" (R. B. Anderson, Ed.), p. 84. Academic Press, New York, 1968.
4. Sillén, L. G., and Martell, A. E., "Stability Constants of Metal-Ion Complexes," Special Publications, Nos. 17 and 25. Chemical Society, London, 1967.
5. Steger, H. F., *Clays Clay Miner.* **21**, 429 (1973).
6. Kerr, G. T., *J. Catal.* **15**, 200 (1969); Jacobs, P. A., and Uytterhoeven, J. B., *J. Chem. Soc. Faraday I* **69**, 373 (1973).
7. Artamanov, V. P., and Pomosov, A. V., *Izv. Vyssh. Ucheb. Zaved, Tsvet. Met.* **16**, 24 (1973).
8. Hepel, T., and Pomianowski, A., *Zesr. Nauk. Univ. Jagiellan Pr. Chem.* **19**, 257 (1974).
9. Van Eyk Van Voorthuysen, J. J. B., and Franzen, P., *Recl. Trav. Chim.* **70**, 793 (1951).
10. Macpherson, H. G., and Livingstone, A., *Miner. Mag.* **39**, 718 (1974).
11. Le Van My, M., *Bull. Soc. Chim. Fr.* 545 (1964).
12. Ward, J. W., *Advan. Chem. Ser.* **101**, 380 (1971).
13. Steinberg, K. H., Bremer, H., Hofmann, F., Minachev, K. M., Dmitriev, R. V., and Detjuk, A. N., *Z. Anorg. Allg. Chem.* **404**, 129, 142 (1974); **407**, 162 (1974).
14. Jacobs, P. A., Van Cauwelaert, F. H., Vansant, E. F., and Uytterhoeven, J. B., *J. Chem. Soc. Faraday I* **69**, 1056 (1973).
15. Eischens, R. P., and Pliskin, W. A., *in* "Advances in Catalysis" (D. D. Eley, W. G. Frankenburg, V. I. Komarewsky and P. B. Weisz, Eds.), Vol. 9, p. 662. Academic Press, New York, 1957.
16. Eischens, R. P., and Pliskin, W. A., *in* "Advances in Catalysis" (D. D. Eley, W. G. Frankenburg, V. I. Komarewsky and P. B. Weisz, Eds.), Vol. 10, p. 1. Academic Press, New York, 1958.
17. Little, L. H., "Infrared Spectra of Adsorbed Species," p. 78. Academic Press, London, 1966.
18. Gentry, S. J., and Rudham, R., *J. Chem. Soc. Faraday I* **70**, 1685 (1974).
19. Levchuk, V. S., and Dzis'ko, V. A., *Kinet Katal.* **10**, 124 (1969).
20. Levchuk, V. S., and Ione, K. G., *Kinet. Katal.* **13**, 949 (1972).
21. Stone, F. S., and Agudo, A. L., *Z. Phys. Chem. (Frankfurt)* **64**, 161 (1969).
22. Butler, J. D., Polis, T. C., and Wood, B. T., *J. Catal.* **16**, 239 (1970).
23. Krylov, O. V., "Catalysis by Non-metals," p. 118. Academic Press, New York, 1970.
24. Ward, J. W., *Trans. Faraday Soc.* **67**, 1489 (1971).
25. Ward, J. W., *J. Catal.* **38**, 351 (1975).